agronomy

MDPI

Article

Molecular Phylogenetic Analysis of Salt-Tolerance-Related Genes in Root-Nodule Bacteria Species *Sinorhizobium meliloti*

Victoria Spartakovna Muntyan and Marina Lvovna Roumiantseva *

Laboratory of Genetics and Selection of Microorganisms, Federal State Budget Scientific Institution All-Russia Research Institute for Agricultural Microbiology (FSBSI ARRIAM), 196608 Saint Petersburg, Russia
* Correspondence: mroumiantseva@yandex.ru; Tel.: +7-(812)-476-28-02

Abstract: A molecular phylogenetic analysis of salt-tolerance-related genes was carried out using complete genome sequencing data available for 26 *Sinorhizobium meliloti* strains and for 25 bacterial strains belonging to 17 genera. It was revealed that the genes of the first and the second stages of the response to salt stress (*aqp*Z, *trk*H, and *trk*A, and *bet*ICBA) have copies of many of the above- indicated genes on pSymA. Data obtained can provide evidence that this replicon, known to be essential for nitrogen fixation rhizobia activity, also has a significant role in the formation of a stress-related gene pool. The closest putative phylogenetic relatives were identified for all 14 tested genes and these are the first insights into the evolutionary pathways for the formation of a stress-related gene pool in root nodule nitrogen-fixing bacteria.

Keywords: *Sinorhizobium meliloti*; molecular phylogenetic analysis; genes related to salt shock; genes related to prolonged salt stress; nucleotide sequences analysis; chromosome; pSymA

check for updates

Citation: Muntyan, V.S.; Roumiantseva, M.L. Molecular Phylogenetic Analysis of Salt-Tolerance-Related Genes in Root-Nodule Bacteria Species *Sinorhizobium meliloti*. *Agronomy* **2022**, *12*, 1968. https://doi.org/10.3390/agronomy12081968

Academic Editor: Enrico Porceddu

Received: 13 July 2022
Accepted: 16 August 2022
Published: 20 August 2022

1. Introduction

Crop production and biodiversity around the world are under threat from a range of environmental constraints, such as salinity, drought and heat stress, which, due to changing climatic conditions, increase the rate of soil erosion and degradation as well as inhibit plant growth and development [1].

Legumes that form a nitrogen-fixing symbiosis with soil saprophytic bacteria have a well-developed root system and can be a promising object for cultivation on arid soils subjected to salinity [2]. Microsymbionts can help to increase plant tolerance to abiotic stress factors and, accordingly, increase plant productivity [2,3]. However, the genetic potential of the microbial component used in the creation of plant–microbial systems based on modern biotechnology methods remains underestimated. In this regard, it may be of interest to study genes related to the tolerance of bacteria to abiotic stress factors, for example, to osmotic and salt types of stress, which adversely affect the vital activity of soil microorganisms.

Salinity is one of the most widespread stress factors; it is also the best-studied factor, since it can be modeled in a laboratory [4]. The reaction of bacterial cells to salt stress is divided into primary and secondary stages (or phase, response and reaction), which are responsible for various proteins/enzymes encoded by both individual genes and groups of genes (hereinafter referred to as stress-tolerance-related genes). The primary reaction of bacteria to salt stress (shock) is associated with the accumulation of water and potassium ions due to passive or active transport through the cell membrane, which has been shown for model objects such as *Escherichia coli* (class: γ-proteobacteria), *Bacillus subtilis* (class: *Bacilli*) and *Pseudomonas aeruginosa* (class: γ-proteobacteria). Multicomponent transporter systems encoded, for example, by the *trk*AH genes and the *kdp*EABCDF operon are responsible for active potassium transport (presented for *E. coli* on Figure 1a; [5,6]). Tolerance to hyperosmotic conditions, especially to soil salinity, is associated with both

osmotic stress, which develops with a lack of water ions, and salt stress, characterized by high extracellular concentrations of cations (for example, sodium) and anions (for example, chloride ions). Aquaporins, which are considered as "water channels", are involved in the passive transport of water ions. These "water channels" are hydrophobic homotetrameric transmembrane proteins of 250–300 aa, which are members of the extensive MIP family (major intrinsic proteins) and often encoded by multicopy (from one to seven) *aqp* genes. It has been shown that aquaporins of phytopathogenic, arbuscular or ectomycorrhizal fungi regulate the membrane permeability not only for water but also for hydrogen peroxide as well as ammonium ions, and they can participate in the development of fungal conidia (virulence and infection processes) [7–9]. The *aqp* genes have also been identified in plants, and their activity can be either constitutive or induced in response to osmotic stress [10], or regulated by hormones or blue light [11,12]. Bacterial porins are actively involved in the enhanced cell growth that occurs in the exponential phase [13–15]. Aquaporins of the peribacteroid membrane of legume symbiosomes, organelles containing differentiated nitrogen-fixing cells of nodule bacteria, are involved in the exchange of metabolites between the host plant and the bacterial microsymbiont, and are known as nodulins (family: Nlm) according to [16,17].

The *aqp* genes in taxonomically unrelated microorganisms may have a low level of similarity; for example, *aqp*Z and *aqp*X in *E. coli* strain K-12 clone MG1655 and *Brucella melitensis* bv. *abortus* 2308, respectively, have a shared identity of 65.26% according to the results of a noncontiguous megablast (discontiguous megablast) [18]. The functional role of the products of these *aqp* genes is also significantly different; for example, AqpX is required under hyperosmotic conditions, while AqpZ is important for protecting cells from hypoosmotic shock [4]. According to data from the literature, the aquaporins of prokaryotes, archaea and eukaryotes differ in the specificity of pores to transferred substrates, according to [19–23]. The secondary stage of the response to salt stress occurs as a result of the accumulation of organic substances, such as trehalose, proline, ectoine, glycine betaine or choline (osmolytes [4,24–26], osmoprotectants [27–29] or osmoprotectors [26,30–32]), in the cytoplasm of bacteria, which is necessary to maintain cell turgor (prolonged exposure to hyperosmotic conditions) [33]. It should be noted that the data discussed above were obtained exclusively for model strains of bacteria from different species, classes or even orders, while for root-nodule bacteria, symbionts of leguminous plants, data about genes involved in the response to salt stress as well as about their functional role are extremely limited.

In the genome of *Sinorhizobium meliloti* strains forming a symbiosis with alfalfa (*Medicago* spp.), genes were identified whose products are similar to genes in *E. coli* involved in the primary response to salt stress (Figure 1b). Among them are the *kdp* operon as well as the *trk*A, *trk*H and *aqp* genes, which are related to the primary response to salt stress. In the genome of the reference strain *S. meliloti* Rm1021, genes *aqp*Z1 and *aqp*Z2 annotated correspondingly on a chromosome (SMc) and on the megaplasmid pSymA, which contains symbiotic genes. The first gene mentioned above encodes the bacterial nodulin-like integral transmembrane protein AqpZ1, presumably involved in the degradation of glycerol compounds as well as in the transfer of glycerol-3-phosphate. However, there are no experimental data confirming the functional role of both of these genes up to now.

In the *S. meliloti* genome, genes involved in the secondary response to hyperosmotic stress were also identified. Such a type of tolerance is linked with the accumulation and synthesis of various osmoprotectors, such as trehalose or glycine betaine. These compounds accumulate at high concentrations via BCCT (betaine/carnitine/choline transporter) transport systems (Figure 1), which are also found in many Gram-negative bacteria [34,35]. Thus, different species of nodule bacteria contained the *tre*AB, *pro*U, *pro*P and *bet*T genes, which are involved in the transport of osmoprotectors. The *tre*Y, *tre*S and *tre*Z genes were also identified in *S. meliloti*, and all of them belong to different potential trehalose synthesis pathways or are involved in the conversion of maltose and maltodextrin, respectively [36]; however, exogenous trehalose transporters, activated in response to salt stress, were not

identified. Glycine betaine (GB or *N*,*N*,*N*-trimethylglycine, or 2-trimethylammonioacetate (IUPAC)) is the most highly effective osmolyte known, the synthesis of which occurs during the two-stage oxidation of choline through the formation of glycine betaine aldehyde [37]. In Gram-positive bacteria such as *Arthrobacter pascens* and *A. globiformis*, as well as in fungi (*Cylindro carpondidymun*), a two-step catalysis of soluble choline oxidase (*cox* and *cod*A genes in *Arthrobacter*, respectively) was studied [38,39]. In *S. meliloti*, the enzymes of the glycine betaine biosynthesis pathway encoded by the *bet*ICBA chromosomal operon were revealed. A similar operon was also described in *Pseudomonas aeruginosa* (PA0031-PA0030-PA0029), as well as in *E. coli* and *Bacillus subtilis*, but the *bet*C gene encoding the synthesis of choline sulfatase was absent in the last two cases [37,40–42]. It has been shown that the *bet*C product is involved in the replenishment of the sulfur pool in *P. aeruginosa*, while in *S. meliloti*, the *bet*C gene encodes choline sulfatase, which hydrolyzes choline-O-sulfate, with the subsequent conversion of choline into glycine betaine [43]. It is important to note that the activity of the *bet* genes in *S. meliloti* is significant in symbiosomes; therefore, it is necessary for benefiting the function of the legume–rhizobium symbiotic system [44–46]. Both types of the above operons have the *bet*I gene, which encodes an HTH-type transcription regulator of the *bet*AB genes in *S. meliloti* and *E. coli*. The *bet*I gene is induced by outside transported choline, for example, from plant root exudates [44]. In alfalfa rhizobia, a homolog of the *bet*B gene (*bet*B2) on the megaplasmid pSymA was identified, whose function is predicted to be a "switch" of the possibility of using GB as a source of carbon or nitrogen in the last stage of glycine betaine biosynthesis [46].

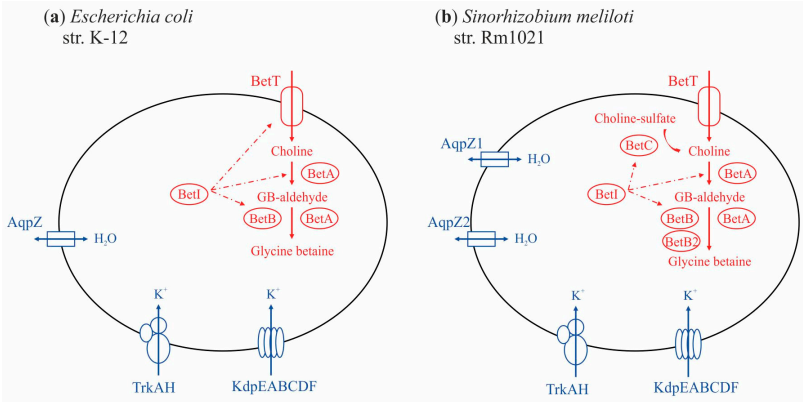

Figure 1. Schematic representation of the osmostress response systems of *E. coli* K-12 (**a**) and *S. meliloti* Rm1021 (**b**). Graphical sketch of osmostress response systems was designed using literature data [33,36,37,43–47]. The presence of BCCT (betaine/carnitine/choline transporter) transport systems are indicated in (**a**,**b**) according [5,35,43–47]. Products of stress-related genes: blue lines indicate primary stage and red lines indicate secondary stage (see the text); AqpZ—aquaporin Z; TrkAH and KdpEABCDF—turgor-responsive uptake transporter systems for K^+; BetT—high-affinity choline import transporter (BCCT transport system); BetA—FAD-containing choline dehydrogenase; BetB—betaine aldehyde dehydrogenase; BetC—choline-O-sulfatase; BetI—transcriptional regulator BetI. Substrates: GB-aldehyde—glycine betaine aldehyde.

Thus, an analysis of the data available in the literature has shown that taxonomically different types of microorganisms have a two-stage response to salt stress, in which both homologous and nonhomologous genes may be involved, the products of which frequently belong to different metabolic pathways. However, it is still impossible to make at least a preliminary characterization of the pool of these genes for the bacteria.

The aim of the presented study was to search for and obtain new knowledge about the abundance of genes known to be involved in the control of stress tolerance (salt tolerance), but little studied in nitrogen-fixing root-nodule rhizobia. The intraspecies diversity of the pool of these genes (presence, copy number and localization in the genome) related to the primary and secondary response of salt stress tolerance (shock and prolonged hyperosmotic

exposure, correspondingly) was studied in this work by evaluating *Sinorhizobium meliloti* strains for which genome-wide data are available. A phylogenetic approach was applied for the first time in order to predict evolutionary pathways for the formation of a stress-related genes pool in root-nodule bacteria, forming a nonobligate mutualistic nitrogen-fixing symbiosis with alfalfa.

2. Materials and Methods

2.1. Complete Genomes

Complete genomes of 51 bacterial strains from 4 classes deposited in GenBank were taken for the research (Table 1).

Table 1. List of bacterial strains.

Class	Genera	Strain[BioSample]	
		Species	GenBank
α-proteobacteria	*Sinorhizobium*	*S. meliloti*	Rm1021[SAMEA3283068], Rm2011[SAMN02603522], USDA1106[SAMN07175168], USDA1157[SAMN07175169], USDA1021[SAMN07175167], B399[SAMN06229775], B401[SAMN06227501], BL225C[SAMN00017103], CCMM B554 (FSM-MA)[SAMN06284128], GR4[SAMN02603224], KH35c[SAMN07175161], KH46[SAMN07175162], HM006[SAMN07175160], M162[SAMN07175163], M270[SAMN07175164], Rm41[SAMN07175165], RMO17[SAMN02952139], RU11/001[SAMEA3146337], SM11[SAMN02603056], T073[SAMN07175166] AK83[SAMN00017059] *, AK21[SAMN08428886] *, AK555[SAMN08826593] *, AK170[SAMN10256575] *, S35m[SAMN16812329] *, CXM1-105[SAMN08826592] *
		S. medicae	WSM419[SAMN02598363]
	Bradyrhizobium	*Brad.* spp.	GAS369[NZ_LT629750.1], ORS 278[SAMEA3138227], USDA 6[SAMD00060992] and USDA 110[SAMN03573437]
	Brucella	*Bruc. melitensis* bv. *abortus*	2308[SAMEA3138256]
	Devosia	*D.* sp.	A16[SAMN04156589]
	Chelativorans	*Chel.* sp.	BNC1[SAMN02598260]
	Agrobacterium	*A. fabrum*	C58[SAMN02603108]
	Rhizobium	*Rh. etli*	CFN 42[SAMN02603106]
	Azorhizobium	*Azor. caulinodans*	ORS 571[SAMD00060925]
	Gluconacetobacter	*Gluc. diazotrophicus*	PA1 5[SAMN02598444]
	Azospirillum	*Azo.* sp.	B510[SAMD00060958]
β-proteobacteria	*Cupriavidus*	*Cupr. taiwanensis*	LMG 19424[SAMEA3138280]
	Azoarcus	*Azoarc.* sp.	BH72[SAMEA3138261]
γ-proteobacteria	*Klebsiella*	*K. pneumoniae* subsp. *pneumoniae*	HS11286[SAMN02602959]
	Escherichia	*E. coli*	K-12[SAMN02604091]
Actinobacteria	*Frankia*	*F.* spp.	ACN14a[SAMEA3138259], EAN1Pec[SAMN02598325], CcI3[SAMN02199398]
	Corynebacterium	*Cor. glutamicum*	ATCC 13032[SAMD00061105]
	Mycolicibacterium	*M. smegmatis*	MC2 155[NZ_LN831039.1]
	Mycobacterium	*M.* spp.	H37Rv[SAMEA3138326], AF2122/97[SAMEA20450668]
	Pimelobacter	*P. simplex*	VKM Ac-2033D[SAMN03009415]

* Strains from collection of Laboratory of Genetics and Selection of Microorganisms of FSBSI ARRIAM deposited in the Russian Collection of Agricultural Microorganisms (RCAM) of FSBSI ARRIAM.

A set of genes for the research was settled up as a result of analysis of published data available for bacteria from different species. Only publications presented practical experiments confirming the participation of one or another gene of interest in the formation

of bacteria stress resistance were selected. Finally, a set of scattered data available for bacteria of 17 genera was obtained. However, not one of those corresponding publications had presented a joint analysis of genes selected for our research. As a result, a group of 14 genes was applied for the research. For bacteria of the species *S. meliloti*, similar data were found only for 8 genes and only for the reference strain Rm1021 (Rm2011); however, these data were also scattered. The main reference object was *E. coli*, since it is for this bacterium that the genes involved in the response to salt shock and prolonged salt stress are most fully described. As a result, we analyzed 396 nucleotide sequences of 14 genes from 51 strains belonging to 18 genera.

2.2. Sequence Similarity Analysis

The homologous genes of interest were chosen based on the data of gene products by using the NCBI Prokaryotic Genome Annotation Pipeline [48] and Prokka [49]. The list of genes involved in primary and secondary stages of salt tolerance of the reference strain *S. meliloti* Rm1021: *trk*A (SMc01046), *trk*H (SMc00937), *trk*H-2 (SMa1691), *kdp*A (SMa2333), *aqp*Z1 (SMc01870), *aqp*Z2 (SMa0627), *bet*I (SMc00095), *bet*I-2 (SMa1414), *bet*B (SMc00094), *bet*B2 (SMa1731), *bet*A (SMc00093), *bet*C (SMc00127). Homology analysis of nucleotide and amino acid sequences was performed by using BlastN and BlastP, respectively. The relative rate of accumulation of substitutions (N) between sequences were calculated by using the formula: $N = L/100 \times n$, where L is the sequence length, and n is the number of substitutions per 100 nucleotides. Nucleotide diversity (Pi) was calculated by the DnaSP v6 software package (ver. 6, Rozas J., Barcelona, Spain [50]), and background rate of evolution was calculated by Ka/Ks ratio, according to [51].

2.3. Phylogenetic Analysis

Multiple nucleotide sequence alignment was performed by Muscle tool [52]; highly variable fragments of the alignments were eliminated by Gblocks program [53]; phylogenetic analysis was performed by IQ-TREE [54] with the Maximum likelihood algorithm (1000 bootstrap replicates), the trees were rendered with Dendroscope3 [55]. Comparative analysis of species trees (based on 16S rDNA nucleotide sequences) and gene trees (based on phylogenetic trees obtained in this work) to identify vertical inheritance and possible events of horizontal gene transfer was carried out using TreeCmp v2.0.76 (ver. 2.0.76, Bogdanowicz D., Gdańsk, Poland [56] and T-REX (Boc A., Montre´al, Canada [57]), which made it possible to calculate normalized distance (matching split distance) between trees for the Yule model and bipartite dissimilarity as an optimization criterion. Bootstrap support in both cases was 1000 replicas.

3. Results

3.1. Genes of the First Stage of the Response to Salt Stress

The *trk*A and *trk*H genes encode proteins of the transmembrane complex (Figure 1). Both genes are activated in the first seconds of the response to salt concentration changes in a growth medium. TrkA of *S. meliloti* is characterized by low-affinity, and it is involved in K^+-uptake pump and in transportation of K^+ at neutral pH under aerobic conditions [58]. In *Escherichia coli*, gene *trk*A is constitutively expressed, and its product is an active K^+/H^+ symporter, operating under similar conditions, but it is ineffective at acidic pH [59]. A secondary point is that in genomes of strains of six different species belonging to alpha, beta and gamma proteobacteria, the *trk*A gene was detected in one copy (Table S1). The same gene was identified in one copy on the chromosome of all 26 tested strains of *S. meliloti*. The sequences of the *trk*A was 1377 bp in majority of studied strains including all *S. meliloti* strains and *Agrobacterium fabrum* str. C58, but only in *Azoarcus olearius* BH72 the length of the same gene was 1404 bp. The *trk*A of *S. meliloti* and *Agrobacterium fabrum* C58 showed 73.71% identity (at Cov = 100% and E-value = 0.0).

It was revealed that *trk*A of *S. meliloti* has no similarity with *trk*A of *E. coli* strain K-12 substr. MG16555 (TrkA *E. coli*/TrkA *S. meliloti* (I = 39.96%, Cov = 99% and E-value = 3 ×

10^{-113}). A phylogenetic analysis of 32 identified *trk*A sequences revealed three groups, A, B and C, which were in a state of "soft" polytomy. This type of polytomy indicates that the division of the phylogenetic tree occurs as a result of insufficient phylogenetic information; furthermore, it shows that the analyzed groups are phylogenetically distinct (Figure 2a; [60–62]). Since each of the three above groups included sequences of strains of one of the three classes (γ-, β- or α-proteobacteria), respectively, it was concluded that the sequences of the genes of interest in the bacteria of each studied class had an independent origin. In group C, which contained sequences of α-proteobacteria strains, there are two monophyletic clades (bootstrap 100%), of which clade C2 included two subclades: C2.1 and C2.2 (bootstrap 74%). Subclade C2.1 contained the *trk*A sequence of strain WSM419 of the closely related *Sinorhizobium medicae* species. The C2.2 included 25 *trk*A sequences of *S. meliloti*, the mean value of the nucleotide diversity of these sequences was rather low (Pi = 0.00335). According to nucleotide substitution frequencies (Ka/Ks), used to predict a background rate of evolution, the *trk*A sequence in *S. meliloti* is under negative selection (Ka/Ks = 0.901982). The applied phylogenetic approach revealed that the *trk*A gene in *S. meliloti* strains (cluster C2.2), as well as in *B. melitensis* bv. *abortus* 2308 (cluster C1) is phylogenetically far from the *trk*A sequences in the studied representatives of γ- and β-proteobacteria (groups A and B). So, *trk*A sequences within α-proteobacteria are phylogenetically distinct and did not have the same origin with γ- and β-proteobacteria.

The *trk*H gene (1455 bp) was found in only half of the tested *S. meliloti* strains; however, almost every second strain had a second copy of *trk*H-2 of the same length located on pSymA (Table S1). Both, *trk*H and *trk*H-2 of *S. meliloti* are encoding TrkH proteins mediating K^+ uptake in bacteria. It was revealed that TrkH allows permeation of K^+ and Rb^+, but not smaller ions such as Na^+ or Li^+ [63]. Additionally, two copies of *trk*H were detected only on the chromosome of *Azorhizobium caulinodans* ORS571 (1407 and 1497 bp), but both sequences were not homologous (identity 83.33%, Cov = 6%, E-value = 3×10^{-6}) and did not show identity with *trk*H or with *trk*H-2 of *S. meliloti* strains. The nucleotide similarity of *trk*H and *trk*H-2 for the reference strain, *S. meliloti* Rm1021, was 75.31% (Cov = 97%, E-value = 0). The identity between *trk*H and *trk*H-2 of *S. meliloti* Rm1021 with *trk*H (1458 bp) of *Agrobacterium fabrum* str. C58 was 68.43% (Cov = 97%, E-value = 2×10^{-149}) and 74.65% (Cov = 98%, E-value = 0.0). Only *trk*H showed similarity with the similar sequence of *E. coli* K-12 substr. MG16555 (I = 74.42%; Cov = 2% and E-value = 0.006). In the remaining three representatives of different species, the *trk*H gene was detected in one copy.

A phylogenetic analysis of 31 sequences of *trk*H homologs revealed three phylogenetic clades, A, B and C, which were in a state of "soft" polytomy (Figure 2b). Clade B united two clusters (bootstrap 99%), of which cluster B2 contained the *trk*H sequence of *S. medicae* WSM419 and the first cluster, B1, included *trk*H-2 sequences identified in *S. meliloti* and *S. medicae* WSM419 strains, as well as a chromosome copy of *trk*H *Azorhizobium caulinodans* ORS571. Nucleotide diversity of *trk*H-2 sequences identified in *S. meliloti* was Pi = 0.01337. Homologs of *trk*H were detected in *Agrobacterium fabrum* C58, *Chelativorans* sp. BNC1, *Brucella melitensis* bv. *abortus* 2308. Clade C included *trk*H (Pi = 0.00194) located on the chromosomes of the studied *S. meliloti* strains. Both copies, *trk*H and *trk*H-2, located on a chromosome and the pSymA of *S. meliloti*, correspondingly, are under affected by negative selection (Ka/Ks = 0.1092). A comparative analysis of the topology of the phylogenetic tree performed on the basis of the nucleotide sequences of 16S rDNA of strains of different species (hereinafter referred to as the reference tree or 16S-PhT) and a tree constructed on the basis of *trk*H sequences (*trk*H-PhT) showed that the latter was also similar to the reference tree insofar as any random trees are similar to each other (normalized distance (matching split distance) in the Yule model = 1.667). This led to the conclusion that the *trk*H sequence located on a chromosome as well as the *trk*H-2 sequence located on the pSymA of *S. meliloti* are phylogenetically unrelated. No horizontal transfer events were detected for the *trk*H and *trk*H-2 genes of *S. meliloti* that occurred from other studied classes of bacteria; at the same time, it might be considered that *trk*H-2 is phylogenetically relative to the *trk*H sequence of *Brucella melitensis* bv. *abortus* 2308.

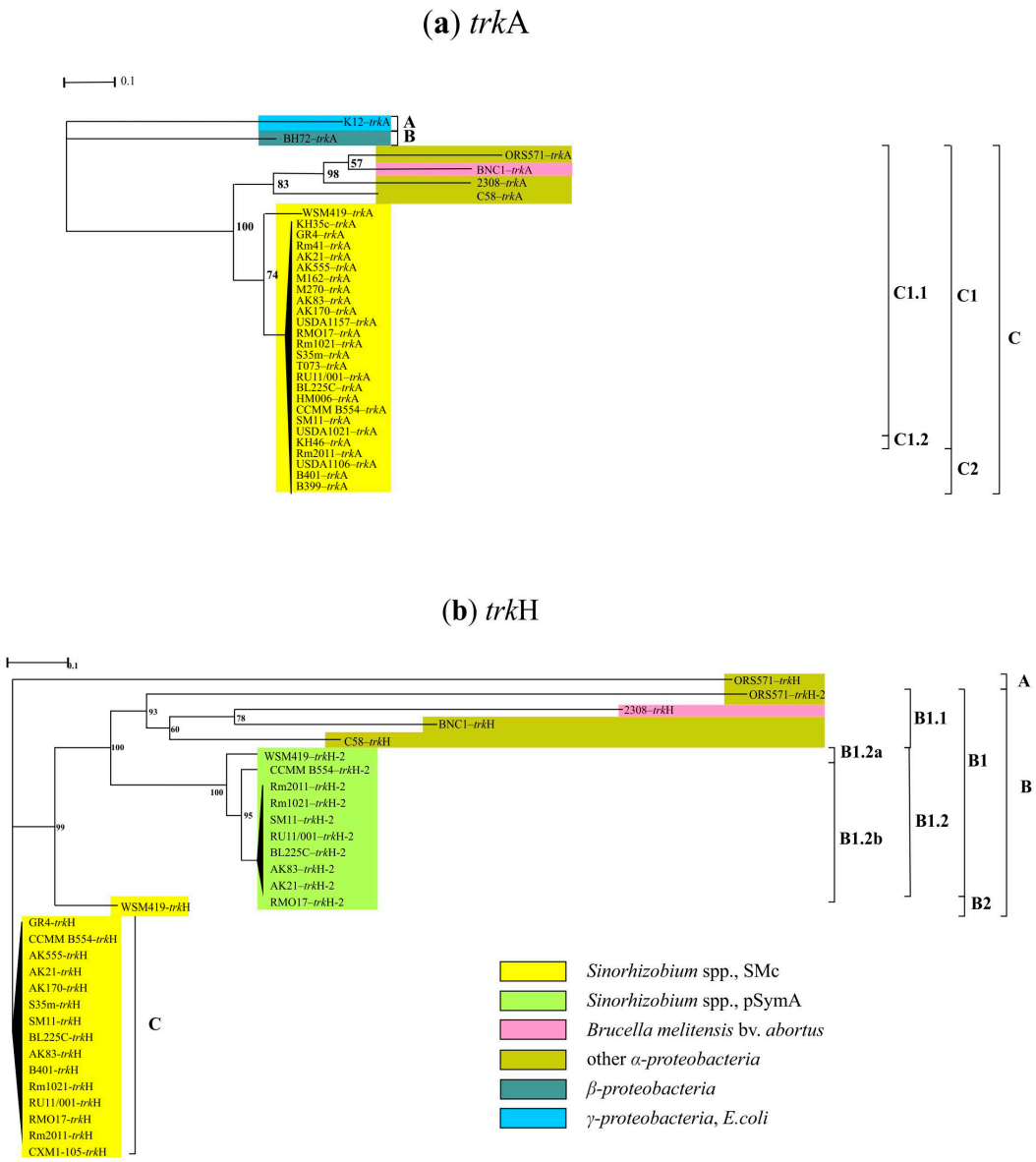

Figure 2. Phylogenetic analysis of *trk*A (**a**) and *trk*H (**b**) genes in α-, β- and γ-proteobacteria, as well *Actinobacteria*. The nucleotide substitution models selected for the analysis were TPM3 + F + G4 for *trk*A sequences and TIM3 + F + G4 for *trk*H ones. The scale bars were 0.1 for *trk*A and *trk*H nucleotide substitutions per site (see Section 2).

The *kdp*EABCD operon's genes are responsible for the synthesis of the Kdp proteins of the ATP-dependent transport system, which is responsible for the accumulation of K^+ under hyperosmotic conditions (Figure 1). In all 26 *S. meliloti* strains, this operon is localized on the pSymA megaplasmid, while in *E. coli*, it is located on a chromosome. The similarity of the nucleotide sequences of each gene of the *kdp*EABCD operon was analyzed in *S. meliloti* as well as *E. coli*. However, the similarity was established for only 31% of the length of the consensus sequences of compared operons (7734 bp and 7677 bp for *S. meliloti* and *E. coli*, respectively; I = 66.69%). Similar operons were found in the many studied representatives of α-, β- and γ-proteobacteria, as well as *Actinobacteria*, but it was not identified in strains that belonged to the following genera: *Brucella*, *Chelativorans*, *Gluconacetobacter* (α-proteobacteria), *Azoarcus* (β-proteobacteria) and *Corynebacteria* (*Actinobacteria*). The *kdp*A gene encodes the potassium-transporting ATPase subunit KdpA, and it was detected in nearly all tested strains (in 46 out of 51) belonging to different species,

with the exception of *Brucella melitensis* bv. *abortus* 2308 (Table S1). Its sequences greatly varied in length (from 1659 bp up to 1818 bp) in the above strains. However, the length of the *kdp*A in *Sinorhizobium*, *Azorhizobium*, *Azospirillum* and *Frankia* (strain EAN1pec) was conserved and was equal to 1710 bp. The identity between *kdp*A from *S. meliloti* Rm1021 and from *Agrobacterium fabrum* str. C58 (1704 bp) did not exceeded 67.85% (Cov = 96%, E-value = 1×10^{-158}).

A phylogenetic analysis of 46 sequences of the *kdp*A gene, encoding the transmembrane subunit KdpA, which is related to the binding and transporting of K^+ ions [4], revealed three clusters in a state of "soft" polytomy. Group A included *kdp*A sequences identified in β-proteobacteria, and group B contained sequences identified in γ-proteobacteria. Group C included sequences identified in both α-proteobacteria and *Actinobacteria*, and had two monophyletic clades (bootstrap 100%). The data obtained supported the presence of a common putative ancestor of the *kdp*A gene homologues for α-proteobacteria (including *S. meliloti*) and *Actinobacteria*. All 26 *kdp*A sequences of *S. meliloti* strains (C-2.2.b.2) were in C-2 (bootstrap 100%). The relative rate of the accumulation of substitutions in sequences of the C-1 clade (class: *Actinobacteria*) as well as in sequences from the subcluster C-2.2.b.2 (*S. meliloti*) was 7.79641 bp for every 100 bp. It was found that the sequences of the *kdp*A gene in *S. meliloti* are under negative selection (Ka/Ks = 0.1317). A comparative analysis of the topology of 16S-PhT and *kdp*A-PhT showed that the normalized matching split distance for the Yule model was 0.8362, indicating that the vertical inheritance of this gene is not obvious. However, 26 horizontal transfers were found (see Materials and Methods), and 20 of them were detected in the studied *S. meliloti* strains. This was supported by the probability of matching the topologies of the 16S-PhT (Figure 3) and *kdp*A-PhT trees (Figure 4a). The facts of the horizontal transfer of the *kdp*A were established within the class *Actinobacteria* (between *Frankia* strains and from *Frankia* to *Mycolicibacterium*); the facts of the transfer of this gene within the class of α-proteobacteria (from *Azospirillum* to *Devosia*, from *Devosia* to *Agrobacterium* and *Bradyrhizobium*) in addition to the probabilities of horizontal transfer events were backed by 100% bootstrap support. In addition, a transfer event of *kdp*A was detected between group C-1 (α-proteobacteria) and group C-2 (*Actinobacteria*), which was confirmed by BD values (131.5%) and bootstrap support (100%). The data obtained allow us to conclude that α-proteobacteria obtained *kdp*A gene from *Actinobacteria* as a result of horizontal gene transfer.

The *aqp*Z gene encoding aquaporin Z was found in the genomes of representatives of eight classes of all the genera under consideration (Table S1). This gene is localized on a chromosome in the analyzed strains belonging to the following genera: *Bradyrhizobium*, *Brucella*, *Devosia* and *Chelativorans* (α-proteobacteria), as well as in a representative of γ-proteobacteria (*E. coli* K-12 substr. MG1655). In 15 strains of *S. meliloti*, the *aqp*Z1 gene located on a chromosome was identified, as was a copy of *aqp*Z2 on the pSymA megaplasmid. In six strains, only the *aqp*Z1 gene was present, while in three strains, only *aqp*Z2 was present, and in two strains, both genes were not detected (Table S1). The size of the *aqp*Z1 and *aqp*Z2 sequences in *S. meliloti* ranged from 615 to 687 bp and from 591 to 699 bp, respectively, while in strains of different species, the *aqp*Z size varied from 591 to 726 bp. The similarity of the nucleotide sequences of *aqp*Z1 and *aqp*Z2 was 82.5% (96% coverage) in *S. meliloti* strains. The two sequences encoding aquaporin Z were determined in the genome of *Agrobacterium fabrum* str. C58. One (*aqp*Z1; 726 bp) of two was localized on the circular chromosome, and the second one (*aqp*Z2; 687 bp) was on the plasmid At. The identity between *aqp*Z1 and *aqp*Z2 was 78.77% (Cov = 99%, E-value = 4×10^{-169}).

The sequence identity between *aqp*Z1 of *S. meliloti* Rm1021 and *aqp*Z1 of *Agrobacterium fabrum* str. C58 was 75.45% (Cov = 96%, E-value = 7×10^{-134}), and between *aqp*Z2 of *S. meliloti* Rm1021 and *aqp*Z2 of *Agrobacterium fabrum* str. C58 it was 72.19% (Cov = 88%, E-value = 5×10^{-98}). There was rather less similarity between the *aqp*Z1 and *aqp*Z2 of *S. meliloti* with *aqp*Z of *E. coli* K-12 substr. MG1655 (64.88 and 63.91%, Cov = 81 and 88%, respectively), but similarity was higher with *aqp*X sequence of *Brucella melitensis* bv. *abortus* 2308 (identity = 70.75% and 71.28%; Cov = 93 and 95%, respectively).

A phylogenetic analysis of 51 *aqp*Z homologues sequences resulted in the three polyphyletic clusters, A, B and C (Figure 4b). Cluster A included the *aqp*Z sequence of *Mycolicibacterium smegmatis* MC2_155 (class: *Actinobacteria*). Cluster B had two clades (bootstrap 65%), of which B-1 included chromosomal and plasmid copies of *aqp*Z of *Agrobacterium fabrum* C58 (bootstrap 93%), suggesting that these copies were obtained as a result of intragenomic recombination. Clade B-2 consisted of two subclades, B-2.1 and B-2.2 (bootstrap 39%), which included sequences from representatives of α- and γ-proteobacteria, respectively. Cluster C had two monophyletic clades (bootstrap 83%), of which clade C-1 combined all the *aqp*Z2 sequences and clade C-2 included sequences of the *aqp*Z1 strains of *S. meliloti*, as well as the *aqp*Z gene of *S. medicae* (bootstrap 94%). The level of identity in the nucleotide sequences of the *aqp*Z1 and *aqp*Z2 of *S. meliloti* is rather high, and both copies are under positive selection (Ka/Ks = 1.1223). These data allow us to predict that both copies may have a dissimilar but essential role in *S. meliloti*.

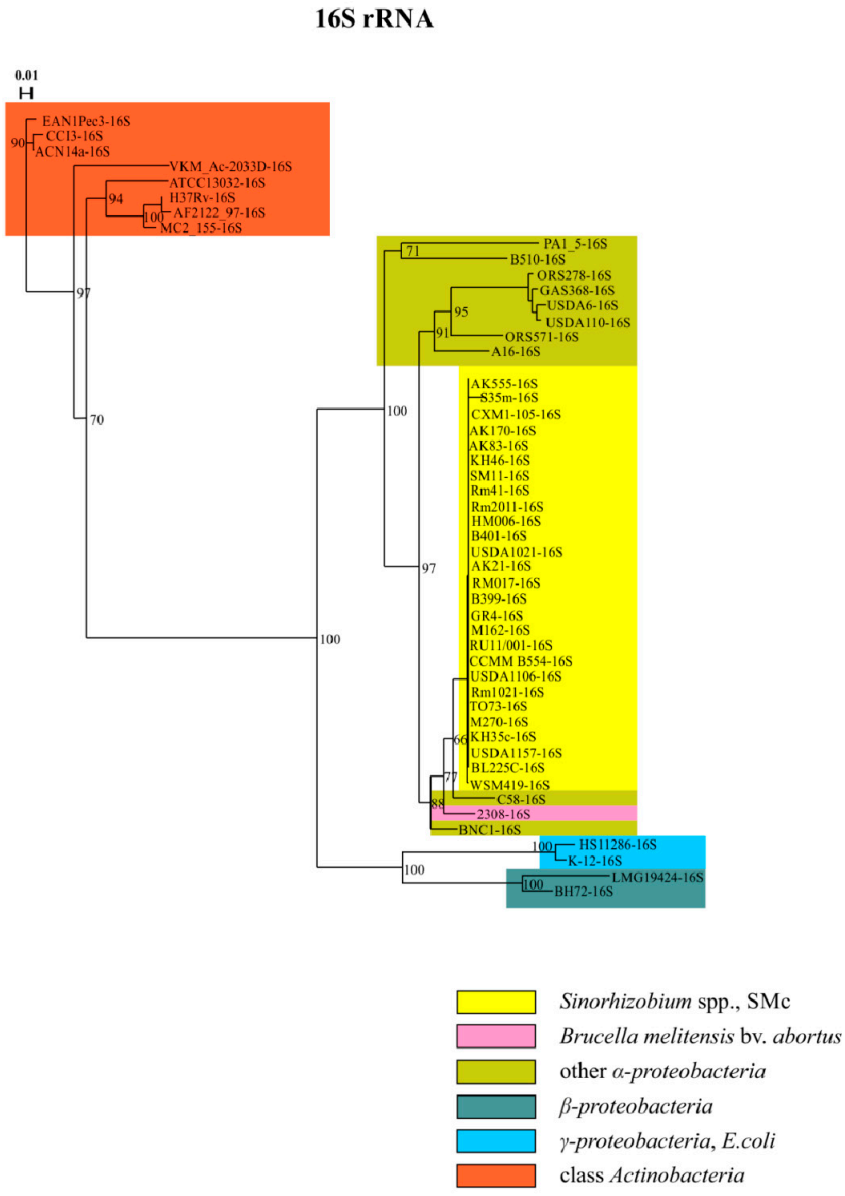

Figure 3. Phylogenetic analysis of 16S rRNA gene sequences in α-, β- and γ-proteobacteria, as well as *Actinobacteria*. The nucleotide substitution model selected for the analysis was TVM + F + G4 for 16S rRNA. The scale bar was 0.01 for 16S rRNA nucleotide substitutions per site.

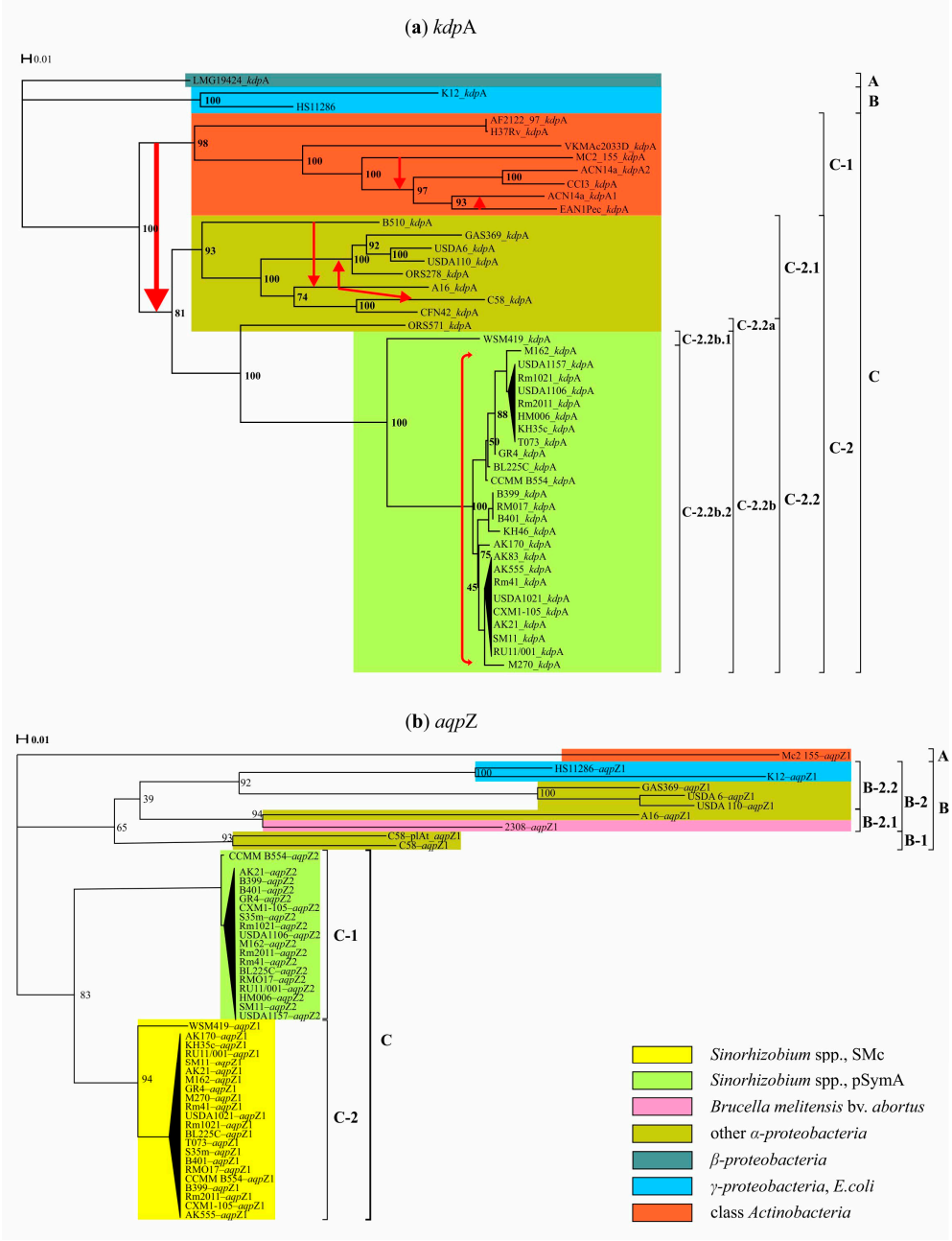

Figure 4. Phylogenetic analysis of *kdp*A (**a**) and *aqp*Z (**b**) gene sequences in α-, β- and γ-proteobacteria, as well as *Actinobacteria*. The nucleotide substitution models selected for the analysis were TVM + F + I + G4 for *kdp*A and TPM3u + F + I + G4 for *aqp*Z. The scale bars were 0.01 for *kdp*A and *aqp*Z nucleotide substitutions per site.

A comparative phylogenetic analysis of the topology of the 16S-PhT and *aqp*Z-PhT showed that the normalized matching split distance to the average value of the Yule model is close to 1 (1.634), which does not allow us to discuss the vertical inheritance of these genes in *S. meliloti*. Moreover, no evidence for the horizontal transfer of *aqp*Z genes in *S. meliloti* was obtained. According to presented data, *aqp*Z sequences abundant in Gram-negative bacteria phylogenetically are far from similar genes in Gram-positive bacteria, but they are closer to sequences determined in slow-growing rhizobia from the genus *Bradyrhizobium*.

Summarizing, it should be noted that both copies of *aqp*Z of *S. meliloti* phylogenetically are far from the corresponding genes of *E. coli*, *Brucella melitensis* (*aqp*X) and *Actinobacteria*. Moreover, AqpZ1 might be involved in sulfur ions transfer in *S. meliloti* as it was concluded

when protein–protein interactions were analyzed using the STRING database [64]. So, *aqpZ* in sinorhizobia is probably involved in cellular processes different from those related to salt stress cell protection, and these genes might be involved in glycerol phosphorylation or sulfur ion transport according to automatic annotation databases (KEGG, BRITE and STRING DB).

3.2. Genes of the Second Stage of the Response to Salt Stress

Homologues sequences of the *bet*I gene, which encoded transcriptional regulator BetI (Figure 1), were detected in tested strains belonged to α- and γ-proteobacteria, but not in representatives of actinobacteria, β-proteobacteria and *Bradyrhizobium* spp. (Table S1). The size of *bet*I sequence varied from 576 to 621 bp in the above strains. Only *S. meliloti* strains harbored besides *bet*I (612 bp) located on the chromosome an additional copy, the *bet*I-2 (612 bp) on pSymA.

No homology between sequences of *bet*I and *bet*I-2 of *S. meliloti* was revealed. Moreover, each of both sequences was distinct from *bet*I of *E. coli* K-12 substr. MG1655. A low level of similarity was observed when amino acid sequences of BetI and BetI-2 of *S. meliloti* were compared (33.52%, Cov = 89%, E-value = 7×10^{-37}), and between both of the above sequences and BetI of *E. coli* K-12 substr. MG1655 (35.42% and 38.1%; Cov = 93%, E-value = 9×10^{-38}; Cov = 92%, E-value = 8×10^{-38}, respectively). The identity between *bet*I of *Agrobacterium fabrum* str. C58 (621 bp) and *bet*I of *S. meliloti* Rm1021 was rather high (73.31%, Cov = 82, E-value = 1×10^{-84}), but no homology was observed with *bet*I-2 (93.33%, Cov = 2%, E-value = 0.046).

A phylogenetic analysis of 59 homologous sequences of *bet*I and *bet*I-2 identified in the genomes of 33 out of 51 strains revealed groups I, II and III, which were in a state of "soft" polytomy with respect to each other (Table S1; Figure 5a). Groups I and II included per one *bet*I-2 sequence of *S. meliloti* GR4 and M270 strains, correspondingly. Group III had two clades (bootstrap 77%). Clade B included six *bet*I-2 sequences of *S. meliloti* and clade A consisted of two subclades (bootstrap 39%; Figure 5a). The A1 subclade contained 16 sequences of *bet*I-2 identified in *S. meliloti*, and the A2 subclade had two clusters (bootstrap 76%). Cluster A2.1 contained the *bet*I-2 sequences of *S. meliloti* AK555 and AK21 strains isolated from the Aral Sea region, subjected to extreme salinity. So, the *bet*I-2 sequences of *S. meliloti* are clustered into five phylogenetically distant clusters, and that may be due to their significant structural differences.

Cluster A2.2 had a subcluster, A2.2b, which included the *bet*I of *Klebsiella pneumoniae* subsp. *pneumoniae* HS11286 and *Escherichia coli* K-12 (substr. MG1655) (from the γ-proteobacterium class). Subcluster A.2.2a united two subgroups, one of which contained five homologues of the *bet*I gene of strains of different genera from the α-proteobacteria class (*S. medicae* WSM419, *Brucella melitensis* bv. *abortus* 2308, *Agrobacterium fabrum* C58, *Rhizobium etli* CFN42, *Azospirillum* spp. BH510). The subsequent descendant division of the A.2.2a-1 cluster resulted in the A2.2a11-2b.2 cluster, which contained the *bet*I sequences of all 26 *S. meliloti* strains, while the *bet*I homologue of *S. medicae* WSM419 was in another cluster A2.2a11-2b.1 (Figure 5a). The *bet*I gene of *S. meliloti* had 65.61% similarity (Cov = 86%, E-value = 6×10^{-25}) with and was phylogenetically closer to the *bet*I gene of *Brucella melitensis* bv. *abortus* 2308 than to the analogous *E. coli* gene. According to the calculated value of the background rate of evolution, both the *bet*I and *bet*I-2 genes of *S. meliloti* are under the influence of negative selection (Ka/Ks = 0.6509). At this stage of the analysis, the putative ancestral sequence of the *bet*I-2 gene located on pSymA was not identified. Phylogenetic and comparative analyses of 16S-PhT and *bet*I-PhT showed that the value of the matching split in the Yule model was 1.667, which made it possible to conclude that horizontal transfer events involving the *bet*I genes were not detected in the analyzed representatives of the *S. meliloti* species. However, the *bet*I-2 homologue appears to have diverged from the putative ancestral sequence earlier than the *bet*I located on the chromosome of *S. meliloti*, as well as its *E. coli* or *B. melitensis* bv. *abortus* homologs, which made it possible to consider the *bet*I-2 of *S. meliloti* as an ancestral sequence.

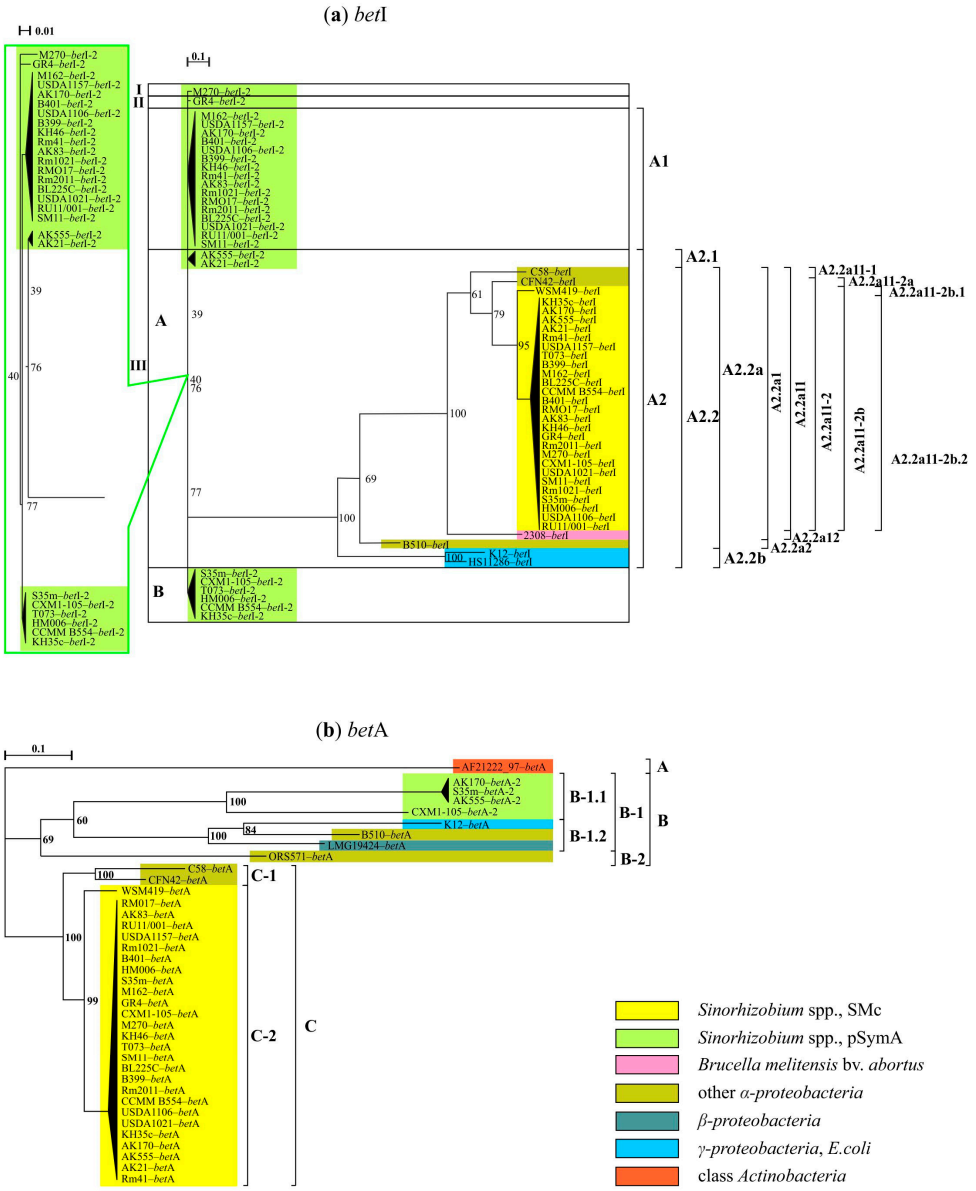

Figure 5. Phylogenetic analysis of *bet*I (**a**) and *bet*A (**b**) genes in α-, β- and γ-proteobacteria, as well as *Actinobacteria*. The nucleotide substitution models selected for the analysis were TPM3u + F + G4 for *bet*I and GTR + F + G4 for *bet*A sequences. The scale bars were 0.1 for *bet*I and *bet*A nucleotide substitutions per site.

The *bet*A gene encoding oxygen-dependent choline dehydrogenase (glucose-methanol-choline (GMC) oxidoreductase family) is involved in the biosynthesis of glycine betaine. The *bet*A gene, represented by one copy on the chromosome, was identified in six out of eleven studied representatives of α- proteobacteria, as well as in β- and γ-proteobacteria, in addition to in a single representative of *Actinobacteria* (Table S1). The size of the *bet*A gene in the studied strains ranged from 1587 to 1713 bp. The value of the nucleotide diversity (Pi) of the *bet*A sequences in *S. meliloti* was 0.00196, while in the other strains mentioned above, it was four times higher (0.00803). Four geographically different strains of *S. meliloti* isolated from different origin centers of alfalfa diversity have a copy of *bet*A-2 on pSymA. The *bet*A-2 sequence size averaged 1626 bp (strains S35m, AK555 and AK170), while in strain CXM1-105 it was shortened (726 bp). The nucleotide diversity of the *bet*A-2 gene (Pi = 0.00597) was three times higher than that of the *bet*A in *S. meliloti*.

Sequences of *bet*A and *bet*A-2 had a low level of similarity (identity 74.21%, Cov = 41% and E-value = 3×10^{-27}); similarly, a low level of shared identity was found between the *bet*A of *S. meliloti* and *E. coli* K-12 substr. MG1655 (identity 63.65%, Cov = 53% and E-value = 2×10^{-21}), and it was not detected in the case of *bet*A-2. The level of similarity for *bet*A-2 of *S. meliloti* and *bet*A (1650 bp) of *Agrobacterium fabrum* str. C58 was low (72.02%, Cov = 37%, E-value = 6×10^{-23}). However, the sequence identity of *bet*A *S. meliloti* and *Agrobacterium fabrum* str. C58 was higher (80.56%, Cov = 99%, E-value = 0.0). An analysis of the ratio of synonymous and nonsynonymous substitutions in the *bet*A and *bet*A-2 nucleotide sequences of *S. meliloti* suggested that both sequences are under negative selection (Ka/Ks = 0.4722).

A phylogenetic analysis was performed for 38 *bet*A homologous sequences detected in 34 strains (Table S1). Identified groups A, B and C were in a "soft" polytomy (Figure 5b). Group A included the only identified *bet*A sequence from a member of the class *Actinobacteria*. Group C consisted of two monophyletic clades (bootstrap 100%), of which clade C-1 contained the *bet*A sequences of *Agrobacterium fabrum* C58 and *Rhizobium etli* CFN42 (bootstrap 100%); clade C-2 included all 26 *bet*A chromosome sequences of *S. meliloti*, as well as *bet*A *S. medicae* WSM419 (bootstrap 99%). Group B consisted of two monophyletic clades (bootstrap 69%), one of which contained the *bet*A sequence *Azorhizobium caulinodans* ORS 571. The second clade included two subclades (bootstrap 60%), one included all *bet*A-2 sequences and the second clade contained *bet*A sequences of representatives of α-, β- and γ-proteobacteria, respectively. Therefore, the *bet*A and *bet*A-2 genes of *S. meliloti* are phylogenetically distant from each other, while the *bet*A-2 sequence is phylogenetically closer to the *bet*A sequence of *E. coli*.

A putative common ancestral sequence for *bet*A of *S. meliloti* and *Agrobacterium fabrum* C58 has been identified. The origin of the *bet*A gene sequences of *S. meliloti* and *E. coli* is later than that of the corresponding *Azorhizobium caulinodans* ORS 571 gene, to which the *bet*A-2 sequence is phylogenetically closer. Phylogenetic and comparative analyses of the 16S-PhT as well as *bet*A-PhT and *bet*A-2-PhT trees showed that the matching split values for the corresponding Yule model were 1.2823 and 1.6236. According to obtained data no events of the horizontal transfer of *bet*A and *bet*A-2 genes occurred, at least among the studied strains.

The *bet*B gene was found in one copy in the genomes of seven out of eleven tested species of α- and γ-proteobacteria, but not among all representatives of β-proteobacteria (Table S1). In all 26 *S. meliloti* strains, in addition to *bet*B, which is in the *bet*ICBA chromosomal operon, a *bet*B2 was identified on pSymA, which is no longer found in the other studied species. Both *bet*B copies of *S. meliloti* encode NAD/NADP-dependent betaine dehydrogenases. The length of *bet*B identified in tested strains varied from 1464 to 2103 bp. *S. meliloti* strains contained *bet*B, which was 1464 bp in length, except strain CXM1-105, in which this sequence was 489 bp, and all strains had *bet*B2 (1470 bp). However, *bet*B and *bet*B2 sequences had a low level of similarity (65.83%, Cov = 97%, E-value = 3×10^{-97}); similarly, a low level of identity was between both *bet*B genes of *S. meliloti* with the *bet*B of *E. coli* K-12 substr. MG1655 (identity: 64.90% and 70.37%; Cov = 74% and 14%; and E-value = 1×10^{-49} and 3×10^{-19}, respectively). The highest level of sequence identity was between *bet*B and *bet*B2 of *S. meliloti* with the *bet*B sequence (1482 bp) of *Agrobacterium fabrum* str. C58 (81.66 and 68.89%, Cov = 98% and 66%, E-value = 0.0 and 1×10^{-81}, respectively).

A phylogenetic analysis of 60 sequences of *bet*B and *bet*B2 identified in 34 strains (Table S1) resulted in two groups, A and B, which were in a state of "soft" polytomy (Figure 6a). Group A included four *bet*B2 sequences from geographically different *S. meliloti* strains: TO73, KH35c, CCMM B554 and HM006. Group B combined two monophyletic clades (bootstrap 100%), of which clade BII included 21 *bet*B2 sequences of *S. meliloti*. Clade BI had two subclades (88% bootstrap), of which subclade BI-1 included only the *bet*B2 sequence of the *S. meliloti* M270 strain and subclade BI-2 combined 34 *bet*B homologs distributed between two clusters (100% bootstrap), in one of which, BI-2a1, *bet*B sequences of *Sinorhizobium* spp. and *Agrobacterium* and *Rhizobium* were combined. Subsequent

descendent clustering showed that all *bet*B sequences identified in 26 *S. meliloti* were in cluster BI-2a1.22b, while the *bet*B homolog of *S. medicae* WSM419 was in cluster BI-2a1.22a (bootstrap 98%; Figure 6a). The *bet*B and *bet*B2 sequences of *S. meliloti* had a level of 71.11% similarity (Cov = 98%, E-value = 0.0), and both genes were phylogenetically more similar to the corresponding gene sequence of *Brucella melitensis* bv. *abortus* 2308 or *Agrobacterium fabrum* str. C58 homologues than to the *E. coli* homologue. An analysis of the ratio of synonymous and nonsynonymous substitutions in the *bet*B and *bet*B2 nucleotide sequences of *S. meliloti* showed that both of these sequences are under negative selection (Ka/Ks = 0.2011). Phylogenetic and comparative analyses of the 16S-PhT as well as the *bet*B-PhT and *bet*B2-PhT trees showed that the matching split distance for the Yule model were 1.2247 and 1.5417, respectively. This allowed for the conclusion that there are no supports for horizontal transfer events of *bet*B and *bet*B2 genes in the tested group of *S. meliloti* strains. Moreover, the presented data evident that the *bet*B2 sequence located on pSymA is a phylogenetically earlier copy compared to the divergent sequence of the *bet*B gene located on a chromosome. A similar origin of the chromosomal copy of *bet*B was suggested in studied representatives from the α- and γ-proteobacteria classes.

The *bet*C gene encodes choline sulfatase, which catalyzes the conversion of choline-O-sulfate into choline, and the crystal structure of BetC (512 aa; pdb 6fny) was determined [65]. Homologs of *bet*C were identified in all of the tested *S. meliloti* strains. The presence of this gene in the closely related species *S. medicae* WSM419, as well as in *Agrobacterium fabrum* C58 and *Rhizobium etli* CFN42 (Table S1), is reported for the first time. In *S. meliloti*, the *bet*C gene is part of the *bet*ICBA chromosomal operon, while in the case of the *Rhizobium etli* CFN42 strain, the *bet*C gene was on the pCFN42e plasmid. Sequence identity between *bet*C (1539 bp) of *S. meliloti* Rm1021 and *bet*C (1512 bp) of *Agrobacterium fabrum* str. C58 was 73.10% (Cov = 99%, E-value = 0.0).

A phylogenetic analysis of 29 *bet*C sequences resulted in three groups, A, B and C, in a "soft" polytomy (Figure 6b). Group A is represented by one *bet*C sequence of *S. medicae*. Group C included *bet*C sequences from *Agrobacterium fabrum* C58 and *Rhizobium etli* CFN42 (identity 78.97%; bootstrap 100%). Group B combined 26 *bet*C sequences identified in *S. meliloti* strains and it had two clades, of which clade B-1 contained the sequence previously described as the "cb" allele according to PCR data [66]. The *S. meliloti* strain, which had this allele, was characterized by a reduced level of salt tolerance and reduced symbiotic efficiency under model salinity conditions. The B-2 clade included two subclades (bootstrap 89%), one of which was the B-2.1 cluster, combining 22 *bet*C sequences of *S. meliloti*, and cluster B-2.2 included *bet*C sequences corresponding to the "ab" allele found in *S. meliloti* strains from geographically different centers of alfalfa diversity [67]. The strains, the sequences of which are presented in subclade B-2.2, had different levels of salt tolerance, but formed an effective symbiosis. Subclade B-2.1 united two monophyletic clusters (bootstrap 51%), of which B-2.1a included 21 *bet*C sequences of *S. meliloti* showing 100% identity with the *bet*C of *S. meliloti* Rm1021, and cluster B-2.1b contained the *bet*C sequence, and the corresponding allele had 98% shared identity with the reference strain. The data obtained show that the *bet*C sequence is conserved in the vast majority of *S. meliloti* strains (Pi = 0.00116), while the *bet*C sequences revealed in native strains adapted to salt stress conditions and isolated from origins of alfalfa diversity are more variable (Pi = 0.00811). The obtained phylogenetic analysis data allowed us to suggest that the *bet*C products of *S. meliloti* and *Agrobacterium fabrum* could perform different functions, which is in agreement with the data [43], but a common ancestor was predicted for both sequences.

Phylogenetic and comparative analyses of the reference tree of 16S-PhT and *bet*C-PhT made it possible to determine the matching split value for the Yule model, which was 1.3307. This made it possible to conclude that horizontal transfer events of the *bet*C gene were not detected in the studied group of strains. Phylogenetic analysis data indicated that the *bet*C gene in *S. meliloti* as well as in closely related *S. medicae* species was introduced from different taxonomic groups; however, a sequence that could be considered ancestral

will be possible to identify with a significant expansion in the number of analyzed genomes and the spectrum of bacterial species.

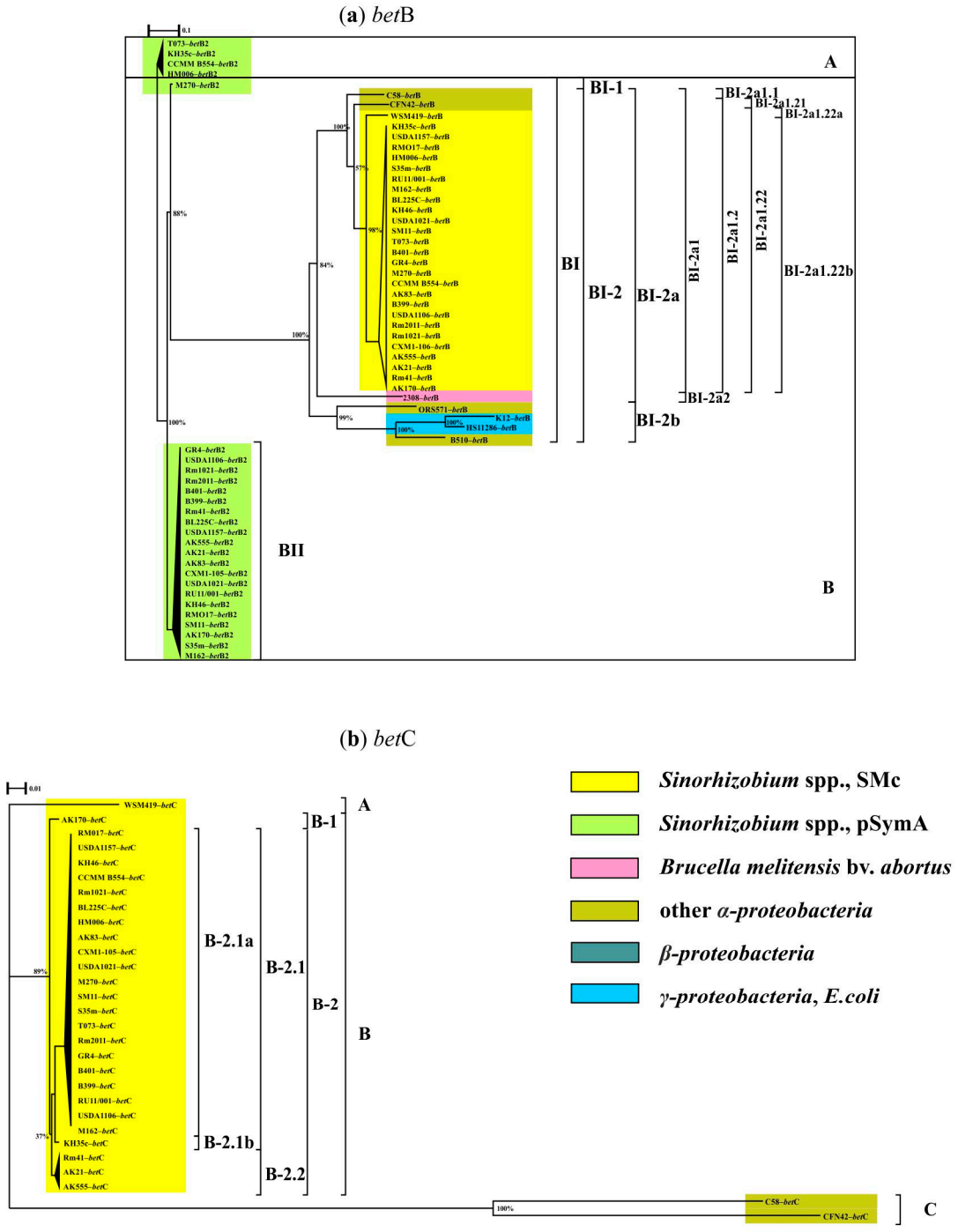

Figure 6. Phylogenetic analysis of *bet*B (**a**) and *bet*C (**b**) genes in α-, β- and γ-proteobacteria, as well as *Actinobacteria*. The nucleotide substitution models selected for the analysis were TVM + F + I + G4 for *bet*B and TVM + F + G4 for *bet*C sequences. The scale bars were 0.1 for *bet*B and 0.01 for *bet*C nucleotide substitutions per site.

4. Discussion

The localization and copy number of the 14 genes involved in the response to salt shock and prolonged salt stress in *S. meliloti* in order to obtain knowledge about a stress-related gene pool formation were determined for the first time. For this purpose, complete

sequenced genomes of the 26 strains (including 4 strains whose genomes were previously sequenced by us [68–71]) were studied. The analysis of *S. meliloti* strains was carried out in comparison with the data obtained by us from the study of the genomes of the other 25 strains from different species belonging to four classes (α-, β- and γ-proteobacteria, as well as *Actinobacteria*).

It was found that the genes involved in the transport of water and potassium (response to salt shock), such as *trk*A and *trk*H, are present in the genomes of representatives of five out of eleven α-proteobacteria species, but are absent in the genomes of slow-growing rhizobia of *Bradyrhizobium* spp. as well as members of the class *Actinobacteria*. The *kdp*A and *aqp*Z genes are present not in all *Bradyrhizobium* spp. and *Actinobacteria* strains. Summarizing, the vast majority of *S. meliloti* strains are harbored in 8 out of 14 studied genes on the chromosome and 6 genes on pSymA, and among the latter, 5 are copies of corresponding chromosomal genes.

The level of shared nucleotide identity of copies and genes with chromosomal localization varied from 66 to 83%, with coverage from varying from 86 to 98%. The level of nucleotide diversity of sequences of copies of the studied genes was basically two times higher. The exception was the *trk*H-2 gene located on pSymA, for which the Pi values were seven times higher and which, as established, is a divergent paralog of the chromosomal *trk*H gene.

The results indicate that the widespread *kdp*A gene, which is part of the *kdp* operon and located on pSymA, is actively involved in interspecific and intraspecific horizontal transfers in the class of α-proteobacteria. This observation is in agreement with data of Anand A. and Sharma A., who reported about *kdp*A gene horizontal transfer for psychrophilic Arctic metagenomes of Pangong Lake [72]. With regard to the *aqp*Z genes involved in the transport of water and various metabolites, we have revealed that plasmid copy was absent two times more often than a chromosomal copy in the genomes of *S. meliloti* strains (frequencies were 0.25 and 0.12, correspondingly). Both *aqp*Z1 and *aqp*Z2, as it was established, have a high level of nucleotide sequence similarity and are under the influence of positive selection; however, it remains unclear to what extent they may differ in functional activity and/or participate in other stressful conditions.

Our phylogenetic analysis showed that the *trk*H and *trk*A genes determined in *S. meliloti* were closer to *Brucella melitensis* bv. *abortus* 2308 than to *E. coli*. At the same time, the *aqp*Z genes of *S. meliloti* are phylogenetically closer to the genes found in slow-growing rhizobia of *Bradyrhizobium* spp. than to the representatives of both of the above species. Our results of the analysis of the widespread *kdp*A gene, which is part of the operon in *S. meliloti*, indicated that it was introduced into α-proteobacteria as a result of horizontal gene transfer from the class *Actinobacteria*.

The secondary response to hyperosmotic stress is associated with the accumulation of osmoprotectors. The *bet*IBA operon, whose gene activity is associated with the synthesis of betaines, is found in many representatives of α-, β- and γ-proteobacteria. In all of the *S. meliloti* strains analyzed, the *bet*ICBA operon is present on the chromosome.

In this research, we have reported for the first time that the *bet*A, *bet*B and *bet*I genes of *S. meliloti* are phylogenetically closer to the corresponding genes of *Agrobacterium* spp., which is genetically relative to *S. meliloti* [73]. Additionally, the *bet*C gene, which was found also in the genomes of *S. medicae* WSM419, *A. fabrum* C58 and *Rh. etli* CFN42, occurred phylogenetically closely related to *S. medicae* species.

Copies of the *bet*I-2 and *bet*B2 genes on pSymA were found in all tested *S. meliloti* strains; hence, copies of the *bet*A-2 genes were identified for the first time in strains isolated from centers of alfalfa diversity (frequency of occurrence 0.02). According to data obtained, plasmid copies of *bet*A-2 and *bet*B2 are phylogenetically closer to the above chromosomal copies, while the regulatory gene *bet*I-2 was phylogenetically closer to the corresponding gene of *Klebsiella pneumoniae* subsp. *pneumoniae* HS11286 (γ-proteobacteria), and, moreover, it is an ancestral sequence for *E. coli* or *B. melitensis* bv *abortus*. Thus, pSymA is an essential replicon not only for nitrogenfixation rhizobia activity, but it also has a

significant role in the formation of a stress-related gene pool. This is in agreement with findings of Galardini et al. [74] that the pSymA megaplasmid contributes to sinorhizobium pangenome expansion.

5. Conclusions

Thus, genes known to be involved in the primary and secondary response to salt stress were studied in full genome-sequenced *S. meliloti* strains in the frame of this research. Protein products encoded by gene copies with chromosomal and plasmid localization may differ in functional role, as was concluded using nucleotide and amino acid polymorphism analysis; however, it is the subject of further research. By phylogenetic approach, the closest phylogenetic predecessors were identified for a set of studied genes, which made it possible to obtain the first ideas about the evolutionary pathways for the formation of a pool of genes related to stress tolerance in root nodule bacteria.

Supplementary Materials: The following supporting information can be downloaded at: https://www.mdpi.com/article/10.3390/agronomy12081968/s1, Table S1: List of genes, detected in the genomes of bacterial strains.

Author Contributions: Conceptualization, V.S.M. and M.L.R.; methodology, V.S.M.; software, V.S.M.; formal analysis, V.S.M. and M.L.R.; investigation, V.S.M. and M.L.R.; writing—original draft preparation, V.S.M. and M.L.R.; writing—review and editing, V.S.M. and M.L.R.; project administration, M.L.R.; funding acquisition, M.L.R. All authors have read and agreed to the published version of the manuscript.

Funding: This paper was produced with support from the Ministry of Science and Higher Education of the Russian Federation in accordance with agreement no. 075-15-2022-320, dated 20 April 2022, on providing grants in the form of subsidies from the federal budget of the Russian Federation. The grant was provided for state support for the creation and development of a World-class Scientific Center, "Agrotechnologies for the Future".

Institutional Review Board Statement: Not applicable.

Informed Consent Statement: Not applicable.

Data Availability Statement: Not applicable.

Conflicts of Interest: The authors declare no conflict of interest.

References

1. Arzani, A.; Ashraf, M. Smart Engineering of Genetic Resources for Enhanced Salinity Tolerance in Crop Plants. *Crit. Rev. Plant Sci.* **2016**, *35*, 146–189. [CrossRef]
2. Zahran, H.H. Legume-Microbe Interactions Under Stressed Environments. In *Microbes for Legume Improvement*; Zaidi, A., Khan, M.S., Musarrat, J., Eds.; Springer International Publishing: Cham, Switzerland, 2017; pp. 301–339. ISBN 978-3-319-59173-5.
3. Roumiantseva, M.L.; Saksaganskaia, A.S.; Muntyan, V.S.; Cherkasova, M.E.; Simarov, B.V. Structural Polymorphism of *Sinorhizobium meliloti* Genes Related to Virulence and Salt Tolerance. *Russ. J. Genet.* **2018**, *54*, 525–535. [CrossRef]
4. Ermilova, E.V. *Molecular Aspects of Prokaryote Adaptation*, 2nd ed.; Khimizdat: St. Petersburg, Russia, 2012; p. 128. (In Russian)
5. Kempf, B.; Bremer, E. Uptake and Synthesis of Compatible Solutes as Microbial Stress Responses to High-Osmolality Environments. *Arch. Microbiol.* **1998**, *170*, 319–330. [CrossRef] [PubMed]
6. Epstein, W. The Roles and Regulation of Potassium in Bacteria. *Prog. Nucleic Acid Res. Mol. Biol.* **2003**, *75*, 293–320. [CrossRef]
7. Dietz, S.; von Bülow, J.; Beitz, E.; Nehls, U. The Aquaporin Gene Family of the Ectomycorrhizal Fungus *Laccaria bicolor*: Lessons for Symbiotic Functions. *New Phytol.* **2011**, *190*, 927–940. [CrossRef]
8. Li, T.; Hu, Y.; Hao, Z.; Li, H.; Wang, Y.; Chen, B. First Cloning and Characterization of Two Functional Aquaporin Genes from an Arbuscular Mycorrhizal Fungus *Glomus intraradices*. *New Phytol.* **2013**, *197*, 617–630. [CrossRef]
9. An, B.; Li, B.; Li, H.; Zhang, Z.; Qin, G.; Tian, S. Aquaporin8 Regulates Cellular Development and Reactive Oxygen Species Production, a Critical Component of Virulence in *Botrytis cinerea*. *New Phytol.* **2016**, *209*, 1668–1680. [CrossRef]
10. Saha, P.; Sade, N.; Arzani, A.; Rubio Wilhelmi, M.D.M.; Coe, K.M.; Li, B.; Blumwald, E. Effects of Abiotic Stress on Physiological Plasticity and Water Use of *Setaria viridis* (L.). *Plant Sci.* **2016**, *251*, 128–138. [CrossRef]
11. Yamada, S.; Katsuhara, M.; Kelly, W.B.; Michalowski, C.B.; Bohnert, H.J. A Family of Transcripts Encoding Water Channel Proteins: Tissue-Specific Expression in the Common Ice Plant. *Plant Cell* **1995**, *7*, 1129–1142. [CrossRef]

12. Kaldenhoff, R.; Kölling, A.; Richter, G. Regulation of the *Arabidopsis Thaliana* Aquaporin Gene *AthH2* (*PIP1b*). *J. Photochem. Photobiol. B* **1996**, *36*, 351–354. [CrossRef]
13. Calamita, G.; Kempf, B.; Bonhivers, M.; Bishai, W.R.; Bremer, E.; Agre, P. Regulation of the *Escherichia coli* Water Channel Gene AqpZ. *Proc. Natl. Acad. Sci. USA* **1998**, *95*, 3627–3631. [CrossRef] [PubMed]
14. Calamita, G. The *Escherichia Coli* Aquaporin-Z Water Channel. *Mol. Microbiol.* **2000**, *37*, 254–262. [CrossRef] [PubMed]
15. Hernández-Castro, R.; Rodríguez, M.C.; Seoane, A.; García Lobo, J.M. The Aquaporin Gene *aqpX* of *Brucella abortus* Is Induced in Hyperosmotic Conditions. *Microbiology* **2003**, *149*, 3185–3192. [CrossRef]
16. Rivers, R.L.; Dean, R.M.; Chandy, G.; Hall, J.E.; Roberts, D.M.; Zeidel, M.L. Functional Analysis of Nodulin 26, an Aquaporin in Soybean Root Nodule Symbiosomes. *J. Biol. Chem.* **1997**, *272*, 16256–16261. [CrossRef] [PubMed]
17. Gavrin, A.; Kaiser, B.N.; Geiger, D.; Tyerman, S.D.; Wen, Z.; Bisseling, T.; Fedorova, E.E. Adjustment of Host Cells for Accommodation of Symbiotic Bacteria: Vacuole Defunctionalization, HOPS Suppression, and TIP1g Retargeting in *Medicago*. *Plant Cell* **2014**, *26*, 3809–3822. [CrossRef]
18. Rodríguez, M.C.; Froger, A.; Rolland, J.-P.; Thomas, D.; Agüero, J.; Delamarche, C.; García-Lobo, J.M. A Functional Water Channel Protein in the Pathogenic Bacterium *Brucella abortus* The GenBank Accession Number for the Nucleotide Sequence Reported in This Paper Is AF148066. *Microbiology* **2000**, *146*, 3251–3257. [CrossRef]
19. Verbavatz, J.M.; Brown, D.; Sabolić, I.; Valenti, G.; Ausiello, D.A.; Van Hoek, A.N.; Ma, T.; Verkman, A.S. Tetrameric Assembly of CHIP28 Water Channels in Liposomes and Cell Membranes: A Freeze-Fracture Study. *J. Cell Biol.* **1993**, *123*, 605–618. [CrossRef]
20. Cheng, A.; van Hoek, A.N.; Yeager, M.; Verkman, A.S.; Mitra, A.K. Three-Dimensional Organization of a Human Water Channel. *Nature* **1997**, *387*, 627–630. [CrossRef]
21. Eskandari, S.; Wright, E.M.; Kreman, M.; Starace, D.M.; Zampighi, G.A. Structural Analysis of Cloned Plasma Membrane Proteins by Freeze-Fracture Electron Microscopy. *Proc. Natl. Acad. Sci. USA* **1998**, *95*, 11235–11240. [CrossRef]
22. Meinild, A.-K.; Klaerke, D.A.; Zeuthen, T. Bidirectional Water Fluxes and Specificity for Small Hydrophilic Molecules in Aquaporins 0–5. *J. Biol. Chem.* **1998**, *273*, 32446–32451. [CrossRef]
23. Hohmann, S.; Bill, R.M.; Kayingo, G.; Prior, B.A. Microbial MIP Channels. *Trends Microbiol.* **2000**, *8*, 33–38. [CrossRef]
24. Yancey, P.H. Organic Osmolytes as Compatible, Metabolic and Counteracting Cytoprotectants in High Osmolarity and Other Stresses. *J. Exp. Biol.* **2005**, *208*, 2819–2830. [CrossRef] [PubMed]
25. Burg, M.B.; Ferraris, J.D. Intracellular Organic Osmolytes: Function and Regulation. *J. Biol. Chem.* **2008**, *283*, 7309–7313. [CrossRef]
26. Tkachenko, A.G. *Molecular Mechanisms of Stress Responses in Microorganisms*; Ural Branch of the Russian Academy of Sciences: Ekaterinburg, Russia, 2012; p. 181. (In Russian)
27. Kempf, B.; Bremer, E. Stress Responses of *Bacillus subtilis* to High Osmolarity Environments: Uptake and Synthesis of Osmoprotectants. *J. Biosci.* **1998**, *23*, 447–455. [CrossRef]
28. Deole, R.; Hoff, W.D. A Potassium Chloride to Glycine Betaine Osmoprotectant Switch in the Extreme Halophile *Halorhodospira halophila*. *Sci. Rep.* **2020**, *10*, 3383. [CrossRef] [PubMed]
29. Nadeem, M.; Ali, M.; Kubra, G.; Fareed, A.; Hasan, H.; Khursheed, A.; Gul, A.; Amir, R.; Fatima, N.; Khan, S.U. Role of Osmoprotectants in Salinity Tolerance in Wheat. In *Climate Change and Food Security with Emphasis on Wheat*; Elsevier: Amsterdam, The Netherlands, 2020; pp. 93–106. ISBN 978-0-12-819527-7.
30. Pinevich, A.V. Microbiology. In *Biology of Prokaryotes*; Publishing House of St. Petersburg State University: St. Petersburg, Russia, 2009; Volume 3, p. 361. (In Russian)
31. Perullini, M.; Amoura, M.; Roux, C.; Coradin, T.; Livage, J.; Japas, M.L.; Jobbágy, M.; Bilmes, S.A. Improving Silica Matrices for Encapsulation of *Escherichia coli* Using Osmoprotectors. *J. Mater. Chem.* **2011**, *21*, 4546–4552. [CrossRef]
32. Stecca, J.D.L.; Martin, T.N.; Lúcio, A.D.; Deak, E.A.; Fipke, G.M.; Bruning, L.A. Inoculation of Soybean Seeds Coated with Osmoprotector in Diferents Soil PH's. *Acta Sci. Agron.* **2018**, *41*, 39482. [CrossRef]
33. Talibart, R.; Jebbar, M.; Gouffi, K.; Pichereau, V.; Gouesbet, G.; Blanco, C.; Bernard, T.; Pocard, J. Transient Accumulation of Glycine Betaine and Dynamics of Endogenous Osmolytes in Salt-Stressed Cultures of *Sinorhizobium meliloti*. *Appl. Environ. Microbiol.* **1997**, *63*, 4657–4663. [CrossRef]
34. Kappes, R.M.; Kempf, B.; Bremer, E. Three Transport Systems for the Osmoprotectant Glycine Betaine Operate in *Bacillus subtilis*: Characterization of OpuD. *J. Bacteriol.* **1996**, *178*, 5071–5079. [CrossRef]
35. Gouffi, K.; Pica, N.; Pichereau, V.; Blanco, C. Disaccharides as a New Class of Nonaccumulated Osmoprotectants for *Sinorhizobium meliloti*. *Appl. Environ. Microbiol.* **1999**, *65*, 1491–1500. [CrossRef]
36. Domínguez-Ferreras, A.; Soto, M.J.; Pérez-Arnedo, R.; Olivares, J.; Sanjuán, J. Importance of Trehalose Biosynthesis for *Sinorhizobium meliloti* Osmotolerance and Nodulation of Alfalfa Roots. *J. Bacteriol.* **2009**, *191*, 7490–7499. [CrossRef] [PubMed]
37. Østerås, M.; Boncompagni, E.; Vincent, N.; Poggi, M.-C.; Le Rudulier, D. Presence of a Gene Encoding Choline Sulfatase in *Sinorhizobium meliloti bet* Operon: Choline-*O*-Sulfate Is Metabolized into Glycine Betaine. *Proc. Natl. Acad. Sci. USA* **1998**, *95*, 11394–11399. [CrossRef] [PubMed]
38. Tani, Y.; Mori, N.; Ogata, K.; Yamada, H. Production and Purification of Choline Oxidase from *Cylindrocarpon didymum* M-1. *Agric. Biol. Chem.* **1979**, *43*, 815–820. [CrossRef]
39. Rozwadowski, K.L.; Khachatourians, G.G.; Selvaraj, G. Choline Oxidase, a Catabolic Enzyme in Arthrobacter Pascens, Facilitates Adaptation to Osmotic Stress in *Escherichia coli*. *J. Bacteriol.* **1991**, *173*, 472–478. [CrossRef]

40. Stover, C.K.; Pham, X.Q.; Erwin, A.L.; Mizoguchi, S.D.; Warrener, P.; Hickey, M.J.; Brinkman, F.S.L.; Hufnagle, W.O.; Kowalik, D.J.; Lagrou, M.; et al. Complete Genome Sequence of *Pseudomonas Aeruginosa* PAO1, an Opportunistic Pathogen. *Nature* **2000**, *406*, 959–964. [CrossRef]
41. Mao, F.; Dam, P.; Chou, J.; Olman, V.; Xu, Y. DOOR: A Database for Prokaryotic Operons. *Nucleic Acids Res.* **2009**, *37*, D459–D463. [CrossRef]
42. Winsor, G.L.; Griffiths, E.J.; Lo, R.; Dhillon, B.K.; Shay, J.A.; Brinkman, F.S.L. Enhanced Annotations and Features for Comparing Thousands of *Pseudomonas* Genomes in the Pseudomonas Genome Database. *Nucleic Acids Res.* **2016**, *44*, D646–D653. [CrossRef]
43. Cregut, M.; Durand, M.-J.; Thouand, G. The Diversity and Functions of Choline Sulphatases in Microorganisms. *Microb. Ecol.* **2014**, *67*, 350–357. [CrossRef]
44. Mandon, K.; Østerås, M.; Boncompagni, E.; Trinchant, J.C.; Spennato, G.; Poggi, M.C.; Le Rudulier, D. The *Sinorhizobium meliloti* Glycine Betaine Biosynthetic Genes (*Bet*ICBA) Are Induced by Choline and Highly Expressed in Bacteroids. *Mol. Plant-Microbe Interact.* **2003**, *16*, 709–719. [CrossRef]
45. Boscari, A.; Van de Sype, G.; Le Rudulier, D.; Mandon, K. Overexpression of BetS, a *Sinorhizobium meliloti* High-Affinity Betaine Transporter, in Bacteroids from *Medicago sativa* Nodules Sustains Nitrogen Fixation During Early Salt Stress Adaptation. *Mol. Plant-Microbe Interact.* **2006**, *19*, 896–903. [CrossRef]
46. Yurgel, S.N.; Rice, J.; Mulder, M.; Kahn, M.L.; Belova, V.S.; Roumiantseva, M.L. Truncated *bet*B2-144 Plays a Critical Role in *Sinorhizobium meliloti* Rm2011 Osmoprotection and Glycine-Betaine Catabolism. *Eur. J. Soil Biol.* **2013**, *54*, 48–55. [CrossRef]
47. Shimada, T.; Ogasawara, H.; Ishihama, A. Single-target regulators form a minor group of transcription factors in *Escherichia coli* K-12. *Nucleic Acids Res.* **2018**, *46*, 3921–3936. [CrossRef] [PubMed]
48. Angiuoli, S.V.; Gussman, A.; Klimke, W.; Cochrane, G.; Field, D.; Garrity, G.M.; Kodira, C.D.; Kyrpides, N.; Madupu, R.; Markowitz, V.; et al. Toward an Online Repository of Standard Operating Procedures (SOPs) for (Meta)Genomic Annotation. *OMICS J. Integr. Biol.* **2008**, *12*, 137–141. [CrossRef] [PubMed]
49. Seemann, T. Prokka: Rapid Prokaryotic Genome Annotation. *Bioinformatics* **2014**, *30*, 2068–2069. [CrossRef] [PubMed]
50. Rozas, J.; Ferrer-Mata, A.; Sánchez-DelBarrio, J.C.; Guirao-Rico, S.; Librado, P.; Ramos-Onsins, S.E.; Sánchez-Gracia, A. DnaSP 6: DNA Sequence Polymorphism Analysis of Large Data Sets. *Mol. Biol. Evol.* **2017**, *34*, 3299–3302. [CrossRef]
51. Korber, B. HIV signature, and sequence variation analysis. In *Computational Analysis of HIV Molecular Sequences*; Rodrigo, A.G., Learn, G.H., Eds.; Kluwer Academic Publishers: Dordrecht, The Netherlands, 2000; Volume 4, pp. 555–572.
52. Edgar, R.C. MUSCLE: Multiple Sequence Alignment with High Accuracy and High Throughput. *Nucleic Acids Res.* **2004**, *32*, 1792–1797. [CrossRef]
53. Talavera, G.; Castresana, J. Improvement of Phylogenies after Removing Divergent and Ambiguously Aligned Blocks from Protein Sequence Alignments. *Syst. Biol.* **2007**, *56*, 564–577. [CrossRef]
54. Nguyen, L.-T.; Schmidt, H.A.; von Haeseler, A.; Minh, B.Q. IQ-TREE: A Fast and Effective Stochastic Algorithm for Estimating Maximum-Likelihood Phylogenies. *Mol. Biol. Evol.* **2015**, *32*, 268–274. [CrossRef]
55. Huson, D.H.; Scornavacca, C. Dendroscope 3: An Interactive Tool for Rooted Phylogenetic Trees and Networks. *Syst. Biol.* **2012**, *61*, 1061–1067. [CrossRef]
56. Bogdanowicz, D.; Giaro, K.; Wróbel, B. TreeCmp: Comparison of Trees in Polynomial Time. *Evol. Bioinform.* **2012**, *8*, 475–487. [CrossRef]
57. Boc, A.; Diallo, A.B.; Makarenkov, V. T-REX: A Web Server for Inferring, Validating and Visualizing Phylogenetic Trees and Networks. *Nucleic Acids Res.* **2012**, *40*, W573–W579. [CrossRef] [PubMed]
58. Cholo, M.C.; Boshoff, H.I.; Steel, H.C.; Cockeran, R.; Matlola, N.M.; Downing, K.J.; Mizrahi, V.; Anderson, R. Effects of Clofazimine on Potassium Uptake by a *Trk*-Deletion Mutant of *Mycobacterium tuberculosis*. *J. Antimicrob. Chemother.* **2006**, *57*, 79–84. [CrossRef] [PubMed]
59. Zakharyan, E.; Trchounian, A. K^+ Influx by Kup in *Escherichia coli* Is Accompanied by a Decrease in H^+ Efflux. *FEMS Microbiol. Lett.* **2001**, *204*, 61–64. [CrossRef] [PubMed]
60. Sayyari, E.; Mirarab, S. Testing for Polytomies in Phylogenetic Species Trees Using Quartet Frequencies. *Genes* **2018**, *9*, 132. [CrossRef]
61. Lin, G.N.; Zhang, C.; Xu, D. Polytomy Identification in Microbial Phylogenetic Reconstruction. *BMC Syst. Biol.* **2011**, *5*, S2. [CrossRef]
62. Maddison, W. Reconstructing character evolution on polytomous cladograms. *Cladistics* **1989**, *5*, 365–377. [CrossRef]
63. Cao, Y.; Jin, X.; Huang, H.; Derebe, M.G.; Levin, E.J.; Kabaleeswaran, V.; Pan, Y.; Punta, M.; Love, J.; Weng, J.; et al. Crystal Structure of a Potassium Ion Transporter, TrkH. *Nature* **2011**, *471*, 336–340. [CrossRef]
64. Szklarczyk, D.; Gable, A.L.; Nastou, K.C.; Lyon, D.; Kirsch, R.; Pyysalo, S.; Doncheva, N.T.; Legeay, M.; Fang, T.; Bork, P.; et al. The STRING Database in 2021: Customizable Protein–Protein Networks, and Functional Characterization of User-Uploaded Gene/Measurement Sets. *Nucleic Acids Res.* **2021**, *49*, D605–D612. [CrossRef]
65. van Loo, B.; Schober, M.; Valkov, E.; Heberlein, M.; Bornberg-Bauer, E.; Faber, K.; Hyvönen, M.; Hollfelder, F. Structural and Mechanistic Analysis of the Choline Sulfatase from *Sinorhizobium meliloti*: A Class I Sulfatase Specific for an Alkyl Sulfate Ester. *J. Mol. Biol.* **2018**, *430*, 1004–1023. [CrossRef]

66. Roumiantseva, M.L.; Belova, V.S.; Onishchouk, O.P.; Andronov, E.E.; Kurchak, O.N.; Chizhevskaya, E.P.; Rumyantseva, T.B.; Simarov, B.V. Polymorphism of *bet*-genes among *Sinorhizobium meliloti* isolates native to gene centers of alfalfa. *Agric. Biol. (Sel'skokhozyaistvennaya Biol.)* **2011**, *3*, 48–54. (In Russian)
67. Roumiantseva, M.L.; Muntyan, V.S. Root Nodule Bacteria *Sinorhizobium Meliloti*: Tolerance to Salinity and Bacterial Genetic Determinants. *Microbiology* **2015**, *84*, 303–318. [CrossRef]
68. Baturina, O.A.; Muntyan, V.S.; Afonin, A.M.; Cherkasova, M.E.; Simarov, B.V.; Kabilov, M.R.; Roumiantseva, M.L. Draft Genome Sequence of *Sinorhizobium meliloti* Strain CXM1-105. *Microbiol. Resour. Announc.* **2019**, *8*, e01621-18. [CrossRef] [PubMed]
69. Baturina, O.A.; Muntyan, V.S.; Cherkasova, M.E.; Saksaganskaya, A.S.; Dzuybenko, N.I.; Kabilov, M.R.; Roumiantseva, M.L. Draft Genome Sequence of *Sinorhizobium meliloti* Strain AK170. *Microbiol. Resour. Announc.* **2019**, *8*, e01571-18. [CrossRef] [PubMed]
70. Muntyan, V.S.; Baturina, O.A.; Afonin, A.M.; Cherkasova, M.E.; Laktionov, Y.V.; Saksaganskaya, A.S.; Kabilov, M.R.; Roumiantseva, M.L. Draft Genome Sequence of *Sinorhizobium meliloti* AK555. *Microbiol. Resour. Announc.* **2019**, *8*, e01567-18. [CrossRef]
71. Muntyan, V.S.; Afonin, A.M.; Vladimirova, M.E.; Saksaganskaya, A.S.; Gribchenko, E.S.; Baturina, O.; Roumiantseva, M.L. Complete Genome Sequence of *Sinorhizobium meliloti* S35m, a Salt-Tolerant Isolate from Alfalfa Rhizosphere in Soil Native to the Caucasus Region. *Microbiol. Resour. Announc.* **2021**, *10*, e01417-20. [CrossRef]
72. Anand, A.; Sharma, A. Use of Proteomics and Transcriptomics to Identify Proteins for Cold Adaptation in Microbes. In *Survival Strategies in Cold-adapted Microorganisms*; Goel, R., Soni, R., Suyal, D.C., Khan, M., Eds.; Springer Singapore: Singapore, 2022; pp. 285–319. ISBN 9789811626241.
73. Wood, D.W.; Setubal, J.C.; Kaul, R.; Monks, D.E.; Kitajima, J.P.; Okura, V.K.; Zhou, Y.; Chen, L.; Wood, G.E.; Almeida, N.F.; et al. The Genome of the Natural Genetic Engineer *Agrobacterium tumefaciens* C58. *Science* **2001**, *294*, 2317–2323. [CrossRef]
74. Galardini, M.; Pini, F.; Bazzicalupo, M.; Biondi, E.G.; Mengoni, A. Replicon-dependent bacterial genome evolution: The case of *Sinorhizobium meliloti*. *Genome Biol. Evol.* **2013**, *5*, 542–558. [CrossRef]